

Simulation of Thin Film Relaxation by Buried Misfit Networks

A. Derardja

Abstract—The present work is motivated by the idea that the layer deformation in anisotropic elasticity can be estimated from the theory of interfacial dislocations. In effect, this work which is an extension of a previous approach given by one of the authors determines the anisotropic displacement fields and the critical thickness due to a complex biperiodic network of MDs lying just below the free surface in view of the arrangement of dislocations.

The elastic fields of such arrangements observed along interfaces play a crucial part in the improvement of the physical properties of epitaxial systems. New results are proposed in anisotropic elasticity for hexagonal networks of MDs which contain intrinsic and extrinsic stacking faults. We developed, using a previous approach based on the relative interfacial displacement and a Fourier series formulation of the displacement fields, the expressions of elastic fields when there is a possible dissociation of MDs. The numerical investigations in the case of the observed system Si/(111)Si with low twist angles show clearly the effect of the anisotropy and thickness when the misfit networks are dissociated.

Keywords—Angular misfit, dislocation networks, plane interfaces, stacking faults.

I. INTRODUCTION

GENERALLY, the interface structures do not result from the exact joining of two lattices and it should necessary inserted the interfacial dislocations to describe this interface which many properties are reliant. Our work is devoted to the study of epitaxial systems with semi coherent interfaces which contain sometimes complex periodic networks of misfit dislocations (MDs). Since the elasticity problem is too difficult in the general case, particular limiting boundary conditions have been considered. For the clarification of such complex surface reconstructions, numerous works have been presented in recent years. Theoretical studies, especially those dealing with isotropic elasticity lead to expressions easy to use (e.g. Bonnet R. [3]).

Similar expressions are obviously impossible to obtain from a formulation based on anisotropic elasticity since it requires numerical solutions. At the same time, quantitative study of image contrast necessitates an exact description of the elastic properties of dislocations. For example, the transmission electron microscopy (TEM) estimation of the vertical magnitude of the contrast distortion due to MDs in very thin films is extremely difficult, since a knowledge of the precise

beam conditions and the elastic properties of the epilayer and substrate is necessary for estimate the vertical magnitude of surface distortion in the TEM data (e.g. Belk and col [4]).

In the literature, it is mentioned that the observed periodic networks of dislocations ended, often, by dissociation. The techniques of high resolution electron microscopy (HREM) and scanning tunnelling microscopy (STM) confirms such hypothesis. Taking the example of the annealed (111) Ni₇₅Pt₂₅ single crystal as observed by STM, computer-generated images depict correlations between the positions of the calculated ditches and subsurface misfit dislocation segments (e.g. Bonnet R. [5]). This author has cited that the surface structures observed by STM may be described as a domain system created by periodically arranged regions with stacking faults and partial dislocations. During the deposition of InAs on GaAs, the junction closes by forming an open triangle from

three partial dislocations ($b = \frac{a}{2} \langle 110 \rangle$), so that the final network is still hexagonal, with alternate open nodes, but enclosed within the partial dislocation triangle is a stacking fault in the (111) growth plane (e.g. Joyce and col. [6]). Also, the STM images given for the InAs/(111) GaAs heteroepitaxy shown that the network of edge dislocations is confined to the interface with no threading component, and is established between 3 and 5 ML InAs thickness, whereupon the slip dislocation systems become active and dominate the surface morphology there-after (e.g. Belk and col [7]). For the low-angle twist boundary Si/(111)Si with a misorientation about 0.5°, an hexagonal network of screw dislocations is expected with Burgers vectors $b = \frac{a}{2} \langle 110 \rangle$.

The dislocation nodes are expected and overlap thus forming a "node network" of dislocation nodes with alternating intrinsic and extrinsic stacking faults (denoted below ISFs and ESFs) (e.g. Föll and col. [2]).

In the present paper, it will be shown that the effect of anisotropy is important and, in principle, the isotropic formulation may not calculate rigorously the elastic fields for some applications.

II. BIPERIODIC ELASTIC FIELDS

Fig. 1 and Fig. 2 depict the Cartesian frame $Ox_1x_2x_3$ used for calculations and the symbols attached to the geometry of the plate like bicrystal for the complex case of dissociated

A. Derardja is with Faculty of Sciences and engineering, University of Batna, 05000, Algeria (e-mail: aderardja@hotmail.com).

dislocations. Point O is in the middle of the hexagonal based pattern UVWRSZ.

The free surface is located at algebraically elevations x_2 denoted h . Vectors \mathbf{a} and \mathbf{c} are the period vectors of the network. The MD pattern is supposed to accommodate simultaneously the interfacial length and/or angular misfits to the two crystals. \mathbf{b}^{ZU} and \mathbf{b}^{UV} are the vectors of Burgers of segments ZU and UV respectively. In the middle of ZU for example the function is equal to $\mathbf{b}^{ZU}/2$ and in the middle of RW it is equal to $-\mathbf{b}^{ZU}/2$.

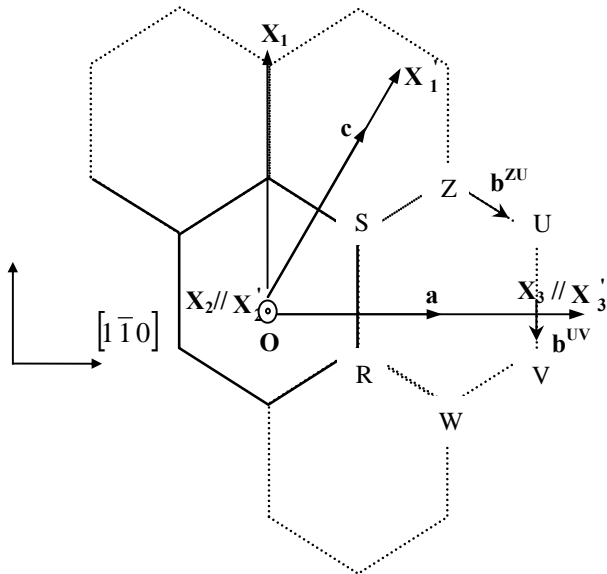


Fig. 1 Geometry of the basic hexagonal cells which constitute the network of MDs, periodic vectors \mathbf{a} and \mathbf{c} . Undissociated nodes. $Ox_1x_2x_3$ is the cartesian frame of calculations and $Ox'_1x'_2x'_3$ is the frame attached to the crystal

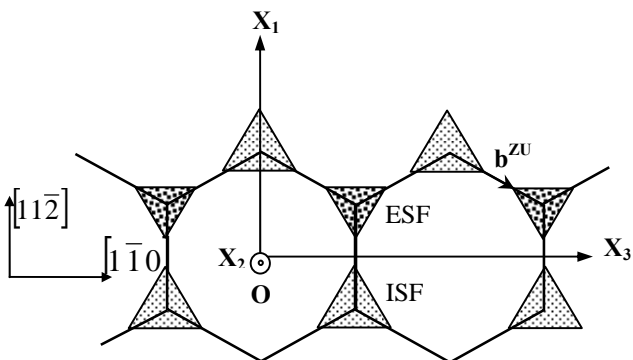


Fig. 2 Geometry of the cells which constitute the network of MDs. The trigonal network is located at the interface ($X_2 = h = 0$ nm)

Relative biperiodic displacement $\Delta \mathbf{u} = \mathbf{u}^+ - \mathbf{u}^- \Big|_{x_2=0}$ is developed in double Fourier series on the whole of the vectors $\mathbf{G} (m, n)$ of the associated reciprocal network.

In the skew frame with unit base vectors (\mathbf{c}, \mathbf{a}) , the relative displacement along the interface is written in indicial notation:

$$\Delta u_K = \mathbf{H}_K^{(0)} + \sum_D \left[\mathbf{H}_K^{(G)} \cos(2\pi \mathbf{G} \times \mathbf{R}) + \mathbf{T}_K^{(G)} \sin(2\pi \mathbf{G} \times \mathbf{R}) \right]$$

$$= \mathbf{H}_K^{(0)} + \sum_{G \neq 0} \frac{1}{2} (\mathbf{H}_K^{(G)} - i \mathbf{T}_K^{(G)}) \exp(2\pi i \mathbf{G} \times \mathbf{R}) \quad (1)$$

Where \mathbf{R} is a vector of the direct lattice, issue from the centre of hexagon and belongs to the interface. \mathbf{G} is the vector of the reciprocal lattice. The position of the apex u of the triangle uvw' along UV (Fig. 3) was selected to specify the extent of dissociation such as:

$$\mathbf{O}u = q\mathbf{c} + (1 - 2q)\mathbf{a} \quad (2)$$

The extension of the dissociation from the node U defined by p , such as: $p = 1 - q$, produces an extra displacement along the triangles within the orientation indicated in Fig. 3, these extra displacements are described respectively by: $-\mathbf{b}_1, \mathbf{b}_2, \mathbf{b}_3, \mathbf{b}_4, \mathbf{b}_5$ et $-\mathbf{b}_6$. This extension may be represented by the surface ratio r defined by: $r = (2 - 3q)^2 / [2 - (3 - q)^2]$.

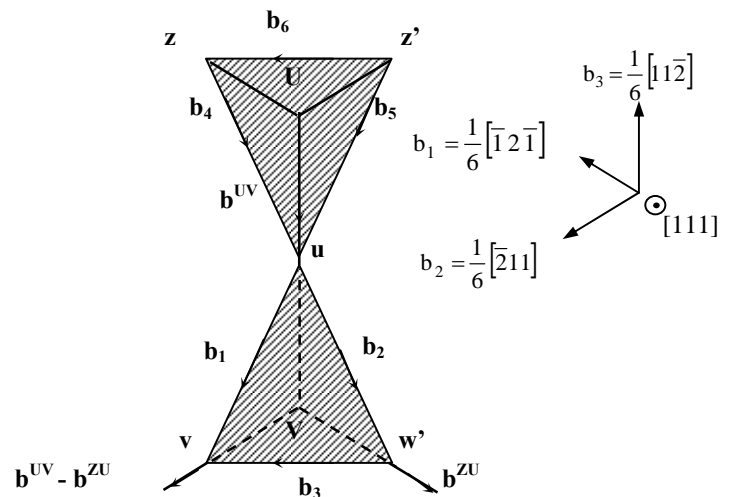


Fig. 3 Geometry of triangular dissociation. Open node V. Partial dislocations having Burgers vectors $\mathbf{b}_1, \mathbf{b}_2$ and \mathbf{b}_3 . Open node U. Partial dislocations having Burgers vectors $\mathbf{b}_4, \mathbf{b}_5$ and \mathbf{b}_6 . The arrows along the lines of dislocations specify their orientations

To represent the complete relative displacements, these extra displacements must be added at those described by the equation (3) for all the points inside the hexagon UVWRSZ.

When the six nodes are dissociated, the Fourier series expressing the final interfacial function $\Delta \mathbf{u}$ is given by:

$$\mathbf{u}^+ - \mathbf{u}^- \Big|_{x_2=0} = \sum_D \left[\begin{aligned} & 2(-\mathbf{b}_1 a_{m,n}^{(1)} + \mathbf{b}_2 a_{m,n}^{(2)} + \mathbf{b}_3 a_{m,n}^{(3)} - \mathbf{b}_4 a_{m,n}^{(4)}) \\ & + \mathbf{b}_5 a_{m,n}^{(5)} - \mathbf{b}_6 a_{m,n}^{(6)} \cos(2\pi \mathbf{G} \times \mathbf{R}) \end{aligned} \right],$$

$$+ \left[\begin{aligned} & \mathbf{T}^{\text{indissociated}} + 2(\mathbf{b}_1 b_{m,n}^{(1)} - \mathbf{b}_2 b_{m,n}^{(2)} - \mathbf{b}_3 b_{m,n}^{(3)} + \mathbf{b}_4 b_{m,n}^{(4)}) \\ & \mathbf{b}_5 b_{m,n}^{(5)} + \mathbf{b}_6 b_{m,n}^{(6)} \sin(2\pi \mathbf{G} \times \mathbf{R}) \end{aligned} \right] \quad (3)$$

A. Displacement Field U_k

As a result, an expression for the displacement field of the MD pattern may be written in a double Fourier series. Using the same conventions and symbols as those given in [8].

$$U_k = 2 \operatorname{Re} \left\{ \sum_D \sum_{\alpha=1}^3 \left[\begin{array}{l} P_{\alpha}^{(G)} \lambda_{\alpha k}^{(G)} \exp \left[2\pi i \left(p_{\alpha}^{(G)} x_2 + \mathbf{GR} \right) \right] + \\ Q_{\alpha}^{(G)} \lambda_{\alpha k}^{(G)} \exp \left[2\pi i \left(p_{\alpha}^{(G)} x_2 + \mathbf{GR} \right) \right] \end{array} \right] \right\} \quad (4)$$

B. Stress Expressions

The derivation of the equation (4) and the application of Hooke's laws lead to the stress expression, which is defined in its compact form by the equation (5). The method used is detailed in [8].

$$\sigma_{kl} = 4\pi \operatorname{Re} \left\{ \sum_D \sum_{\alpha=1}^3 \left[\begin{array}{l} i L_{\alpha kl}^{(G)} P_{\alpha}^{(G)} \exp 2\pi i (\mathbf{GR} + p_{\alpha} x_2) \\ + i L_{\alpha kl}^{(G)} Q_{\alpha}^{(G)} \exp 2\pi i (\mathbf{GR} + p_{\alpha} x_2) \end{array} \right] \right\} \quad (5)$$

C. Limiting Boundaries Conditions

- i The displacement field \mathbf{u} is biperiodic and parallel to the interface. It is discontinuous through the interface, aside from the centres of the cells of the hexagonal networks. The discontinuity of \mathbf{u} along the interface noted $\Delta \mathbf{u}$ is relatively complex to formulate analytically in the case of the dissociation, but it can be written under its compact form as follow:

$$\Delta \mathbf{u} \Big|_{x_2=0} = \sum_{\mathbf{G} \neq 0} \frac{1}{2} \left[(\mathbf{H}_{\mathbf{k}} - i\mathbf{T}_{\mathbf{k}}) \exp(2\pi i \mathbf{GR}) \right] \quad (6)$$

In the expression (6), the vectors \mathbf{T} and \mathbf{H} are depends only of the geometry of the MD lines and their Burgers vectors.

- ii Continuity of the stresses σ_{2k} at the interface

The condition of the equilibrium of the interface is satisfied when the components of the normal stresses are equal to zero:

$$\sigma_{2k}^+ \Big|_{x_2=0} = \sigma_{2k}^- \Big|_{x_2=0} \quad (7)$$

- iii Zero applied stress σ_{2k} at the free surface :

For $x_2 = h$, the normal stresses σ_{2k}^+ are zero.

$$\sigma_{2k}^+ \Big|_{x_2=h} = 0 \quad (8)$$

After tedious developments of the limiting boundary conditions, a system of 9×9 complex equations is obtained with 9 unknown coefficients. This system can not, be solved analytically. The solution of the linear system has been found by a numerical inversion of the system. In this context, a double precision Fortran programme of calculations is written to evaluate the anisotropic elastic fields and give the distortion

of the free surface whatever be the nano-thickness of the layer. This method turned out to be rigorous for the study of any geometry of MD networks.

III. APPLICATION

The image Fig. 4 obtained by Föll is the basis of this application. It illustrates the dissociated hexagonal network into ISFs and ESFs respectively in the interface of a Si/(111)Si low-angle twist boundary. This interphase boundary Si/(111)Si separates an epilayer whose thickness is denoted h and a substrate. The layer is slightly disorientated in torsion compared to the substrate of an angle $\beta = 0.5^\circ$ around the axis Ox_2 perpendicular to the interface. The initial hexagonal network of dislocations whose period is $a = c = 10$ nm is dissociated in all its triple nodes of partials of Shockley delimiting alternatively intrinsic and extrinsic stacking faults. The elastic anisotropic fields are determined and the curves simulate the state of the free surface describing the extent of the dissociation of the nodes.

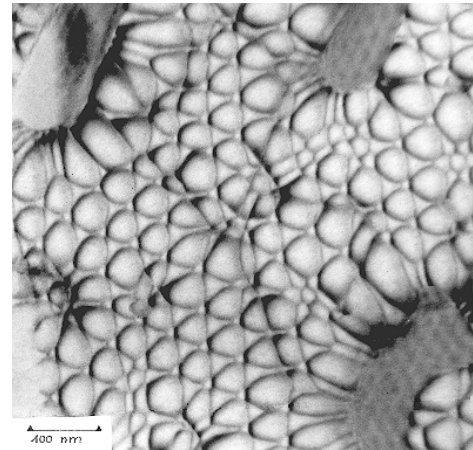


Fig. 4 Low twist boundary on {111} plane imaged with STM. It shows contrast from the stacking faults in the intrinsic nodes (the extrinsic nodes are in good contrast)

IV. RESULTS AND DISCUSSION

In reference to the work achieved by Bonnet [5] which treats the same model in isotropy, we plotted, in quasi isotropy, the curve of the free surface elevation in function of the dissociation. The curves of Fig. 5 (a) and Fig. 5 (b) are represented for a thickness of the layer equal to 4 monolayers. The results are similar to those obtained in isotropy. Indeed, when the curve of Fig. 5 (b) and the curve obtained by Bonnet, in the isotropic case, for the annealed (111) $Ni_{75}Pt_{25}$ single crystal are analysed, it is noteworthy that the shape of the curve traced in quasi-isotropy is in conformity, which makes it possible to conclude a validation of the calculation program. The elevation is less important in quasi-isotropy than in anisotropy. It is really impressive that the difference which exists in term of elevation to the top in the FEI (node V) and in the FEE (node U) is about 0.02 nm when the network is completely dissociated ($p=q=1/2$). The evolution of this

elevation according to the dissociation of nodes U and V reports two states different from surfaces under jacentes generated by the dissociation of the MDs in partial of Shockley limiting alternately intrinsic and extrinsic faults described by the orientation of vectors b_1, b_2, b_3 and b_4, b_5, b_6 respectively.

The contrast of each image is brighter for high elevations. Fig. 6 (c) exhibits star like contrasts when ISF's and ESF's are equally present ($p=q=1/2$). For this particular case, the numerical image is similar to the Fig. 4. It is important to note that the points of the tops of the triangles are not perfectly superposed. It can be explain discreetly by the fact that the dissociation is determined by an energy balance between the stacking faults. The experience shows that, really, the energy of the FEE exceeds that of the FEI (e.g. Hirth [9]). In Consequences, the effect of anisotropy is far from being negligible; and the isotropy may not give the precision expected for some applications.

Also, it is notable to know that the present method may also apply to regular networks for which the surface layers have a chemical nature different from that of the substrate and heteroepitaxial systems.

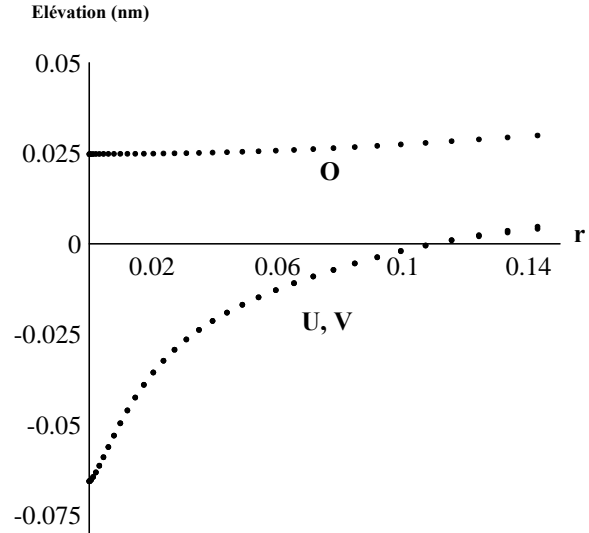
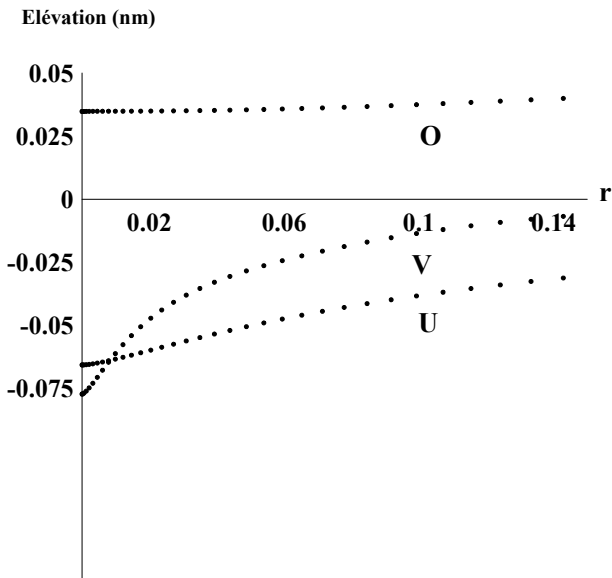
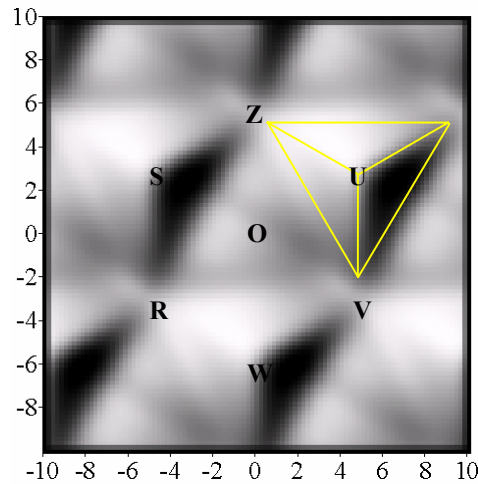


Fig. 5 Change of the free surface elevation directly above points O, U and V in function of the surface ratio r , when the extensions of the ISF's and ESF's increase simultaneously

The images represented on the Fig. 6 are numerical simulations and are equivalents to the STM images. They describe the effect of the extent of the dissociation on the deformation of the free surface. It is found that when the node U is not dissociated ($q = 1/3$ and $p 2/3$), the FEI situated at the level of the point V is completely separated in a triangle well determined. On the other hand, when the node U is dissociated (a), the FEE seems a little bit vague in contrast (b) but she is defined well when the outline is stage fright.



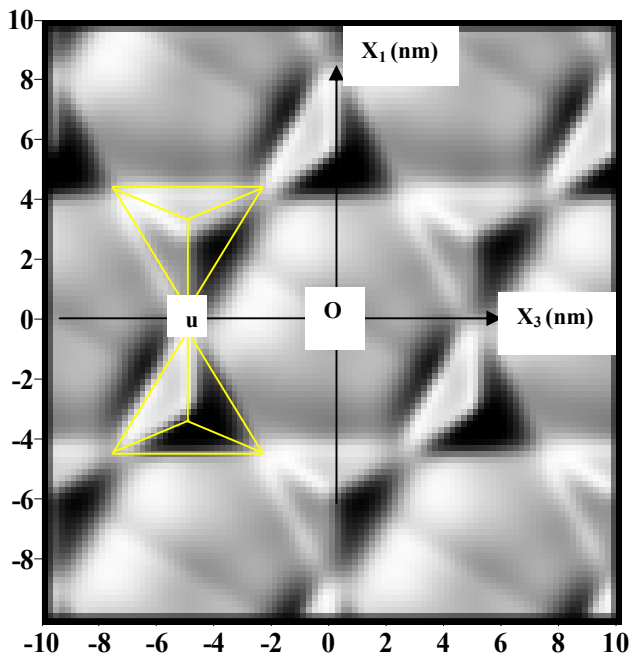
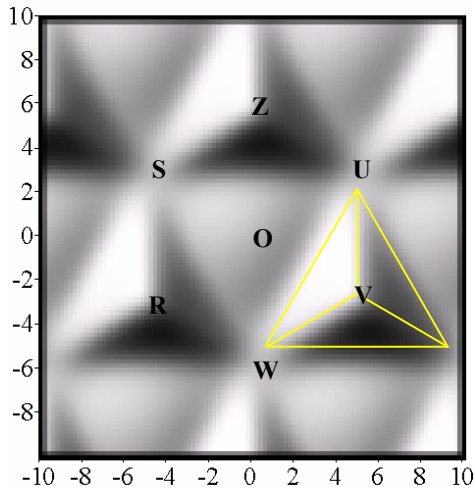


Fig. 6 Examples of calculated free surface relief of Si/(111)Si. The white (black) contrasts correspond to bumps (ditches) of the free surface. The thickness of the epilayer is 4 monolayers

It is known that in the techniques of epitaxy, the epitaxial stresses relax generally by introduction of dislocations or by the propagation of the dislocations pre-existent. The relaxation is realized progressively with the thickness of the layer deposited. The Fig. 7 described the topologies of the free surface in the planes (x_2, x_3) and (x_2, x_1) , for thicknesses of the epilayer between 4 and 20 mono layers and for a coefficient of dissociation $p = q = 1/2$. It appears on the point $x_1 = x_3 = 0$ in the plane (x_2, x_3) and for a thickness $h = 4$ mono layers a light tension related to the value of the vector b_1 . This tension is vanished entirely for $h = 6$ mono layers.

Our aim is to determine the critical thickness of this system. In effect, for $h = 20$ mono layers, the magnitude of the distortions is less than 0,001 nm. For $h = 30$ mono layers, there is no deformation of the free surface.

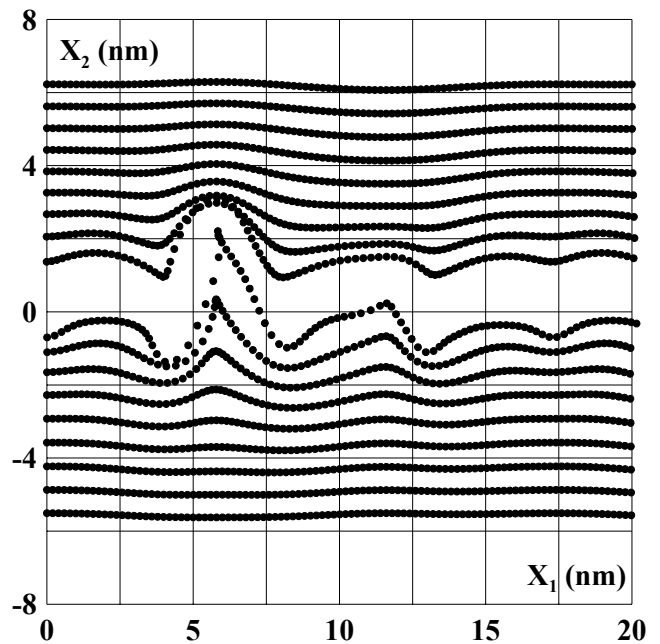
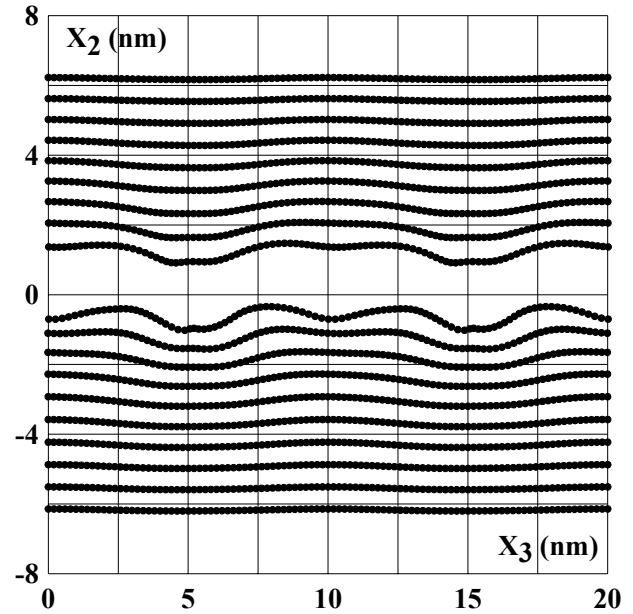


Fig. 7 Topologies of the free surfaces for a thicknesses $h = 2, 4, 6, 8, 10, 12, 14, 16, 18$ and 20 monolayers and for an equal dissociation ($p = q = 1/2$)

V. CONCLUSION

The scope of this application is twofold: first, the limit of the calculations in isotropic elasticity is obviously shown. Second, STM images observed by Föll and col. are simulated and the elastic fields determined with precision.

REFERENCES

- [1] Derardja A., Adami L., Benyoussef S. and Bonnet R., Anisotropie de la relaxation elastique d'un reseau biperiodique de dislocations: theorie et application aux bicristaux de semi-conducteurs, Ann. Chim. Sci. Mat, Vol 29(4), 123-132, 2004.

- [2] Föll H. et Ast D., TEM observations on grain boundaries in sintered silicon, *Phil. Mag.A*, Vol 40, 598-610, 1979.
- [3] Bonnet R., Topographic effect of themisfit dislocation dissociation in threefold symmetry epitaxial systems, *Phil. Mag. A*, vol 79, 1909-1922, 1999.
- [4] Belk J. G., Sudijono J. L., Zhang X. M., Neave J. H., Jones T. S. And Joyce B. A., Surface contrast in two dimensionally nucleated misfit dislocations in InAs / GaAs(110) heteroepitaxy, *Phys. Rev. Lett.*, Vol 78, 475, 1997.
- [5] Bonnet R, Evaluation of surface strain due to the reconstruction of atomically close-packed crystalline surfaces, *Phys. Rev. B*, Vol 61, 14059-14065, 2000.
- [6] Joyce B. A., Jones T. S. and Belk J. G., Reflection high-energy diffraction/scanning tunnelling microscopy study of InAs growth on the three low index orientations of GaAs: Two-dimensional versus three-dimensional growth and strain relaxation, *J. Vac. Sci. Techno. B*, Vol 16, 2376, 1998.
- [7] Belk J. G., Surface aspects of strain relaxation during InAs/GaAs heteroepitaxy, Ph. D. thesis, Imperial College, University of London, 1997.
- [8] Outtas T., Adami L., Derardja A., Madani S. and Bonnet R., Anisotropic elastic field of a thin bicrystal deformed by a biperiodic network of misfit dislocations, *Phys. Stat. Sol.(a)*, Vol 188, 1041-1045, 2001.
- [9] Hirth J.P. and Lothe J., *Theory of dislocations*, second edition (New York: Wiley), 375, 1982.
- [10] Bourret A. and Fuoss P. H., Solving an interface structure by electron microscopy and x-ray diffraction: The GaAs(001)-CdTe(111) interface, *Appl. Phys. Lett.* Vol 61, 1034-1036, 1992.
- [11] Romanov A. E., Petroff P. M. And Speck J. S., Lateral ordering of quantum dots by periodic subsurface stressors, *App. Phys. Lett.*, Vol 74, 2280-2282, 1999.
- [12] Coelho J., Patriarche G., Glas F., Sagnes I. and Saint-Girons G., Dislocation networks adapted to order the growth of III-V semiconductor nanostructures, *physica status solidi (c)*, Vol 2, 1933 – 1937, 2005.
- [13] MRS Symposium Proceedings Series, Nanostructured Interfaces, San Francisco, editor: 506 Keystone drive, Warrendale, PA 15086-7573 USA, Vol 727, 2002 MRS Spring Meeting.
- [14] Fournel F., Moriceau H., Magnea N., Eymery J., Rouvière J. L., Rousseau K. and Aspar B., Ultra thin silicon films directly bonded onto silicon wafers, *Mat. Sci. And Engineering, B* 73, 42-46, 2000.
- [15] Fournel F., Moriceau H., Magnea N., Eymery J., Rouvière J. L., Rousseau K. and Aspar B., Accurate control of the misorientation angles in direct wafer bonding, *Applied Physics Letters-* Vol 80, 793-795, 2002.
- [16] Renaud G., Ducruet M., Ultrich O. and Lazzari R., Apparatus for real time in situ quantitative studies of growing nanoparticles by grazing incidence small angle X-ray scattering and surface differential , *Nuclear Instruments and Methods in Physics Research Section B: Beam Interactions with Materials and Atoms.* Vol 222, 667-680, 2004.
- [17] Zheleva T., Ichimura M., Oktyabrsky S. and Narayan J., Atomic scale characterization of InGaAs/GaAsSi heterostructure by HREM, atomistic modeling and multislice image simulation, *Semicond. Charac.(Int. Workshop)*, Conférence en 1995, éditeurs: Bullis et col., Imprimeur : AIP Press, Woodbury, N. Y., USA, 688-692, 1996.
- [18] Rouviere J. L., Rousseau K., Fournel F. and Moriceau H., Hudge difference between low and high angle twist grain boundaries: the case of ultrathin (001) Si films bonded to (001) Si Wafers, *App. Phys. Lett.*, Vol 77, 1135- 1137, 2000.
- [19] Bott M., Hohage M., Michely T. and Comsa G., *Phys. Rev. Lett.*, 70, 1993, 1489.
- [20] Nakajima K., Calculation of stresses in strained semiconductor layers, *Mater. Res. Soc. Symp. Proc.* 338, 149-160, 1994.
- [21] Gutkin M. Y. and Romanov, K. N. Mikaelyan and Ovid'ko I. A., Generation and evolution of partial misfit dislocations and stacking faults in thin-film heterostructure, *Physics of the solid State*, Vol 43, 42-46, 2001.